

The direct observation of ferromagnetic domain of single crystal CrSiTe₃

Shenghang Wu, Lihai Wang, Bin Gao, Yazhong Wang, Yoon Soek Oh, Sang-Wook Cheong, Jiawang Hong, and Xueyun Wang

Citation: *AIP Advances* **8**, 055016 (2018); doi: 10.1063/1.5024576

View online: <https://doi.org/10.1063/1.5024576>

View Table of Contents: <http://aip.scitation.org/toc/adv/8/5>

Published by the *American Institute of Physics*

Articles you may be interested in

[Electrical-field-induced magnetic Skyrmion ground state in a two-dimensional chromium tri-iodide ferromagnetic monolayer](#)

AIP Advances **8**, 055316 (2018); 10.1063/1.5030441

[Strong spin-lattice coupling in CrSiTe₃](#)

APL Materials **3**, 041515 (2015); 10.1063/1.4914134

[Texture-enhanced Al-Cu electrodes on ultrathin Ti buffer layers for high-power durable 2.6 GHz SAW filters](#)

AIP Advances **8**, 045212 (2018); 10.1063/1.5017091

[Spin-orbit torque induced magnetic vortex polarity reversal utilizing spin-Hall effect](#)

AIP Advances **8**, 055314 (2018); 10.1063/1.5028342

[On the radiated EMI current extraction of dc transmission line based on corona current statistical measurements](#)

AIP Advances **8**, 055001 (2018); 10.1063/1.5018328

[The effect of surface wettability on the performance of a piezoelectric membrane pump](#)

AIP Advances **8**, 045010 (2018); 10.1063/1.5017993

AIP | Conference Proceedings

Get **30% off** all
print proceedings!

Enter Promotion Code **PDF30** at checkout



The direct observation of ferromagnetic domain of single crystal CrSiTe₃

Shenghang Wu,^{1,2} Lihai Wang,³ Bin Gao,^{4,5} Yazhong Wang,⁴
Yoon Soek Oh,^{4,6} Sang-Wook Cheong,^{3,4} Jiawang Hong,¹
and Xueyun Wang^{1,a}

¹School of Aerospace Engineering, Beijing Institute of Technology, Beijing 100081, China

²School of Mathematics and Physics, University of Science and Technology Beijing, Beijing 100083, China

³Laboratory for Pohang Emergent Materials and Max Plank POSTECH Center for Complex Phase Materials, Pohang University of Science and Technology, Pohang 790-784, Korea

⁴Rutgers Center for Emergent Materials and Department of Physics and Astronomy, Rutgers University, Piscataway, New Jersey 08854, USA

⁵Department of Physics, Rice University, Houston, Texas 77005-1827, USA

⁶Department of Physics, Ulsan National Institute of Science and Technology, Ulsan 44919, Republic of Korea

(Received 2 February 2018; accepted 7 May 2018; published online 15 May 2018)

Layered van der Waals interacting system that can be exfoliated to few layers are promising for exploring fundamental physics with rich electronic and optical properties. Combining the emerging phenomenon with long-range magnetic orders could lead to novel potential ultra-compact spintronics. Recently, CrXTe₃ (X=Ge, Si) were reported that can persist magnetism after being exfoliated to few layers, however the magnetic domain structure in layered or bulk single crystal has remained unexplored. Here we choose CrSiTe₃ single crystal as a model system, combining low-temperature magnetic force microscope, to demonstrate the magnetic domain structure, as well as the domain evolution in the presence of magnetic field, which is consistent with the magnetic behaviors measured by Magnetic Properties Measurement System (MPMS). Our result gives a simple portray of the magnetic properties of single crystal CrSiTe₃, which provides a basis for the future research on magnetic layered van der Waals interacting system in potential application at 2-dimensional limit. © 2018 Author(s). All article content, except where otherwise noted, is licensed under a Creative Commons Attribution (CC BY) license (<http://creativecommons.org/licenses/by/4.0/>). <https://doi.org/10.1063/1.5024576>

The past decade has witnessed the rapid development of 2-Dimensional (2D) materials with interlayer van der Waals interaction.^{1–6} Due to their fascinating properties with novel physics and potential applications in devices, researchers start to search and investigate more layered materials with additional ferroic orders, such as ferroelectricity and ferromagnetism.^{7–12} These materials are expected to exhibit more fascinating behaviors after exfoliated to monolayer/few layers.¹³ Recently, layered van der Waals (vdW) interacting magnetic semiconductors such as CrXTe₃ (X=Ge, Si) and CrI₃ were discovered,^{14–17} which has attracted enormous attentions, due to the existing of intrinsic ferromagnetism in the exfoliated monolayer/few layers. Such long-range ferromagnetic order results from the magnetic anisotropy.¹⁸ These discoveries demonstrate layered vdW crystals like CrXTe₃ and CrI₃ could be useful for studying fundamental spin behaviors and in many technologies from sensing to data storage.¹⁹

Though the magnetic response in few layers CrGeTe₃ has been demonstrated by magneto-optic Kerr microscopy,¹⁶ the magnetic domain distribution in layered or bulk single crystal has yet been investigated. Especially the magnetic domain evolution in the presence of magnetic field,

^aCorresponding author: xueyun@bit.edu.cn

which provides a solid foundation of the future studies on single-layer CrXTe_3 . Here, in this letter, we choose CrSiTe_3 as a model system, to demonstrate the direct observation of ferromagnetic domains and related evolution in the presence of magnetic field in bulk single crystal by using low-temperature Magnetic Force Microscope (MFM). The magnetic properties is also confirmed by Magnetic Properties Measurement System (MPMS).

Single crystals of CrSiTe_3 were grown by a flux method. High purity element Cr (99.99%), Si (99.99%), and Te (99.99%) were mixed in a molar ratio of 2:6:36; the extra Si and Te were used as flux. The materials were placed in an alumina crucible, then sealed in an evacuated quartz tube. The tube was heated to 700 °C, held for 2 days and then slowly cooled to 500 °C over a period of 1 day. Then the tube was placed in a centrifuge to remove the flux. The resultant platelet single crystals are a few millimeters in size and have a metal luster. The XRD data is shown in Fig. 1(a). Inset image displays the CrSiTe_3 single crystal.

CrSiTe_3 crystallized in $R\bar{3}$ space group, which is a layered material. The top view of the crystal structure is displayed in Fig. 1(b). The distance between layers is 3.3 Å, leading to a similar cleavage energy as graphene. This property ensures the feasibility of exfoliation. Each unit cell comprises three CrSiTe_3 layers stacked in an ABC sequence, with alternately arranged Te-Cr-Te and Te-Si-Te sandwiches. The Cr^{3+} ions are located at the center of a distorted octahedron of six Te atoms, while the two Si atoms form a pair and located between two adverse Te triangles. So the Cr^{3+} ions and Si pairs, are in a 2:1 ratio when sandwiched between Te planes, as Fig. 1(c) shown. The magnetic property results from the magnetic moments of Cr^{3+} , which ferromagnetic aligned parallel to the c -axis, as shown by the black arrows in Fig. 1(c). Moreover, the strong anisotropic 2D Ising-like behavior is confirmed by neutron scattering experiment.²⁰

The magnetic properties are confirmed by MPMS, including the temperature-dependent magnetic susceptibility and magnetic hysteresis. All measurements of magnetic properties $M(H)$, $\chi_{DC}(T)$, were performed in a Quantum Design MPMS-XL7. Fig. 2(a) shows the temperature variation of DC magnetic susceptibility χ in zero field-cooled (ZFC) process for the magnetic field both parallel and perpendicular to the c axis. The evolution of χ with temperature and bigger magnitude along the c axis are consistent with the transition to the ferromagnetic order at $T_c=33$ K, with spins sitting along the c axis, which is also confirmed by the field dependence of magnetization measured at 5 K, as displayed in Fig. 2(b). The saturation moment at 5 K approximately equals to 3 μB , which agrees

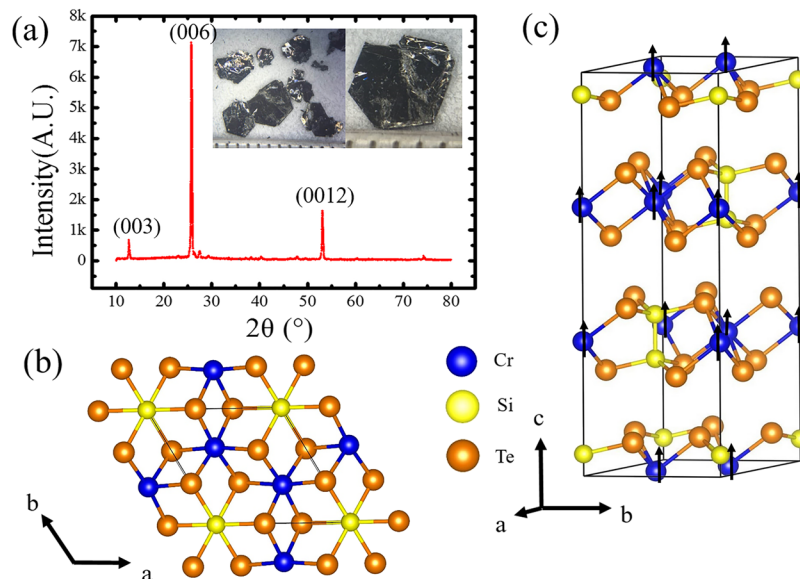


FIG. 1. XRD data and crystal structure of CrSiTe_3 . (a) XRD data shows (003), (006) and (0012) planes of CrSiTe_3 , the inset is images of single crystals with shining ab -plane surfaces. Schematic of crystal structure: (b) View of the ab -plane of a single CrSiTe_3 layer. (c) Crystal cell of CrSiTe_3 single crystals, the magnetic spin is indicated by the black arrow.

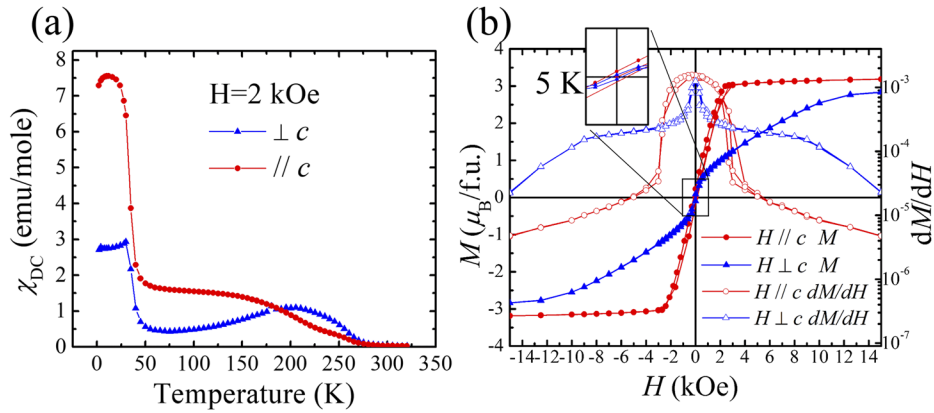


FIG. 2. (a) Temperature dependence of DC magnetic susceptibility χ_{DC} in zero field-cooled (ZFC) process along two crystallographic directions, parallel and perpendicular to the c axis, in $\mu_0 H = 0.2$ T. (b) Magnetic field dependence of magnetization $M(H)$ along two crystallographic directions, parallel and perpendicular to the c axis at 5 K.

with the expected value of $3 \mu_B$ for high spin configuration state of Cr^{3+} . The remanent magnetization is $0.23 \mu_B$ for $H \parallel c$, and $0.0925 \mu_B$ for $H \perp c$ respectively. The coercive field is 4 Oe for $H \parallel c$ and 68 Oe for $H \perp c$ respectively. Both the magnetic susceptibility and the magnetic hysteresis indicate the magnetic anisotropy in $CrSiTe_3$ system, which is consistent with the previous work.¹⁸

The evolution of magnetic domain structures on the ab -plane is taken by using Attocube low temperature scanning probe microscope, which enables us to do scanning in the temperature range 4 K to 300 K. The AFM was operated in helium exchange gas, in dual pass tapping mode with lift height 50 nm. Magnetic force microscope (MFM) images were obtained in units of phase shift. The phase change of the cantilever's oscillation is precisely measured by a fiber-based optical interferometer as illustrated in Fig. 3(a). The magnetic field of up to 8 T can be applied along the c -axis direction, which is normal to the sample surfaces. Commercial MFM tip were used. $CrSiTe_3$ single crystal samples were cleaved in air before being loaded into the low-temperature AFM, thus the sample surface is atomically flat for magnetic signal scanning.

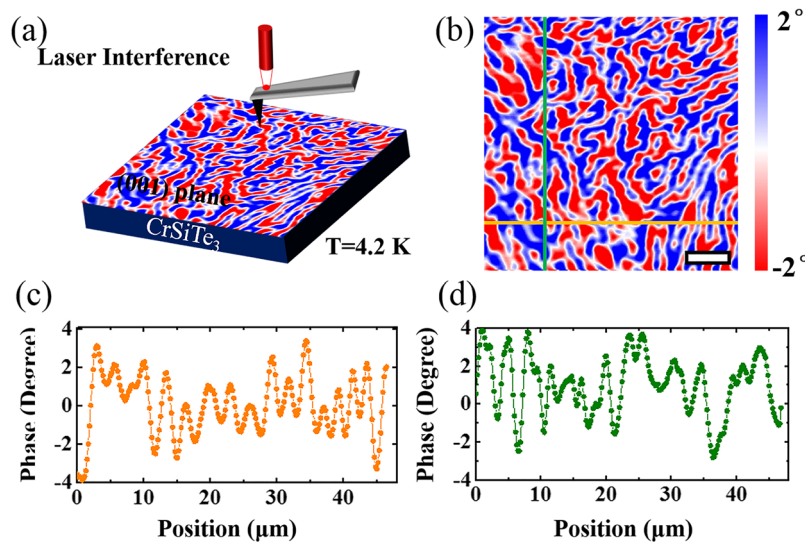


FIG. 3. (a) Schematic of the dual pass MFM, the phase change of the cantilever results from the magnetic force gradient is precisely measured by using a fiber-based optical interferometer (b) The spontaneous formed domain structure in the (001) plane of single crystal $CrSiTe_3$. The scale bar is $10 \mu m$ (c) and (d) local phase variation along two orthogonal directions presented in two different colors.

To observe the spontaneous formation of magnetic domain pattern in bulk CrSiTe_3 . We first map the magnetic domain pattern in (001) plane of CrSiTe_3 single crystal in the absence of magnetic field at 4.2 K. As Fig. 3(b) shows, the magnetic domain is distributed in a maze-like pattern, with red and blue presenting two different spin orientations. By analyzing the area of domain distribution, the upward and downward domains are in half-half ratio. In Fig. 3(c) and (d), the local phase variations along two orthogonal directions within the plane are presented, indicating the randomly distributed upward and downward magnetic domains.

The domain evolution is imaged in the presence of sweeping magnetic fields up to 3 kOe in a smaller scanning area. Two different locations of the sample are detected, labeled as Area 1 and 2, respectively. At area 1, the magnetic field is ramping from 0 kOe to 3 kOe, with 1 kOe step. When applied magnetic field is zero, the area of domains with upward and downward spins are almost equally distributed, as Fig. 4(a) displays, and the phase contrast is consistent with Fig. 3(b). As the magnetic field increases, the domains with the spin along the applied magnetic field start expanding as the red colored area increase (Fig. 4(b–d)). Note that the applied magnetic field is point out of the sample surface, thus the red (blue) domain indicates the upward (downward) spin orientation. At 3 kOe, as shown in Fig. 4(d), the single domain indicates the magnetic saturation, which is consistent with the magnetic hysteresis measurement. In order to see the evolution details, we applied a magnetic field ramping from 1 kOe to 2 kOe at area 2, with variable finer steps, as shown in Fig. 4(e–h). Such a multi-domain to single domain evolution can be explained by the motion of the domain walls as we increase the magnetic field. An interesting behavior is deserved to be emphasized that the wavy domain walls between upward and downward magnetic domains become smoother as the magnetic field increases. Meanwhile, when the applied magnetic field reaches to the saturation field, the domain distribution changes from maze-like to separated worm-like behavior with bubble domains. When the magnetic field is removed, the domain distribution is randomly restored with equally upward and downward magnetic domains, which indicates the nucleation of the magnetic domains has no obvious pinning effect in CrSiTe_3 single crystals.

In conclusion, we used MPMS and low temperature MFM to measure the magnetic properties of a CrSiTe_3 single crystal. The temperature dependent magnetic susceptibility curve and H/M hysteresis at 5 K are acquired. MFM scanning was performed to map the magnetic domain revolution in the presence of variable magnetic field. The result of the domain evolution is consistent with the magnetic hysteresis with a saturation field of 3 kOe. The maze-like domain pattern melt down and finally form a single domain when the applied field is sufficient. Our results may help to portray the overall

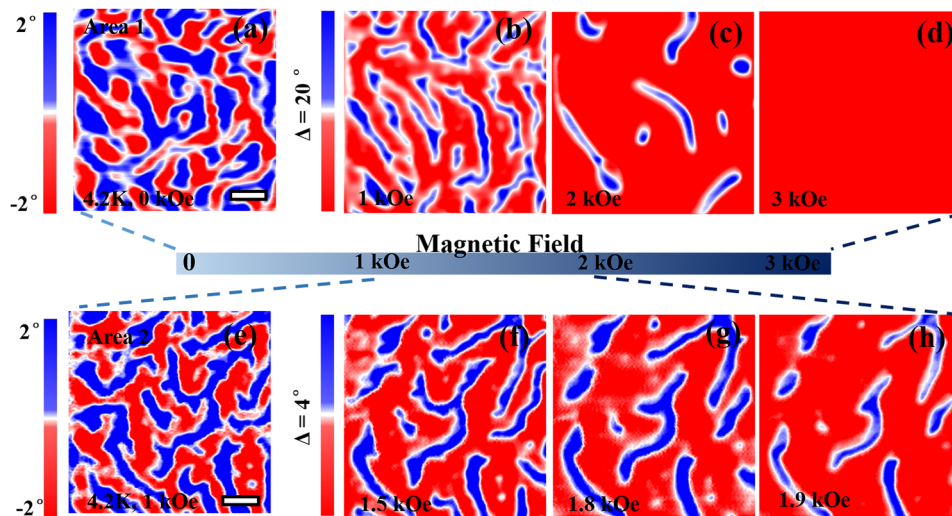


FIG. 4. Evolution of the magnetic domain structures, the scale bar is 5 μm . (a-d) shows the area 1 with a magnetic field sweeping from 0 kOe to 3 kOe, with 1 kOe step. Area 2 (e-h) is applied with a magnetic field sweeping from 1 kOe to 2 kOe to show a detailed magnetic domain revolution.

magnetic property of bulk CrSiTe₃ and provide a foundation of the future 2D magnetic semiconductor research.

The authors acknowledge the fruitful discussion with Houbing Huang and Xue Fei. X.W. acknowledges the National Natural Science Foundation of China (Grant No. 11604011). J.H. is funded by the National Science Foundation of China (Grant No. 11572040) and the Thousand Young Talents Program of China. The work at Rutgers University was supported by the NSF under Grant No. DMR-1629059.

- ¹ K. S. Novoselov, A. K. Geim, S. V. Morozov, D. Jiang, Y. Zhang, S. V. Dubonos, I. V. Grigorieva, and A. A. Firsov, *Science* **306**(5696), 666–669 (2004).
- ² K. S. Novoselov, A. K. Geim, S. V. Morozov, D. Jiang, M. I. Katsnelson, I. V. Grigorieva, S. V. Dubonos, and A. A. Firsov, *Nature* **438**(7065), 197–200 (2005).
- ³ A. K. Geim and K. S. Novoselov, *Nature Materials* **6**(3), 183–191 (2007).
- ⁴ S. Z. Butler, S. M. Hollen, L. Cao, Y. Cui, J. A. Gupta, H. R. Gutierrez, T. F. Heinz, S. S. Hong, J. Huang, A. F. Ismach, E. Johnston-Halperin, M. Kuno, V. V. Plashnitsa, R. D. Robinson, R. S. Ruoff, S. Salahuddin, J. Shan, L. Shi, M. G. Spencer, M. Terrones, W. Windl, and J. E. Goldberger, *ACS Nano* **7**(4), 2898–2926 (2013).
- ⁵ A. K. Geim and I. V. Grigorieva, *Nature* **499**(7459), 419–425 (2013).
- ⁶ J. A. R. S. Das, M. Dubey, H. Terrones, and M. Terrones, *Annu. Rev. Mater. Res.* **45** (2015).
- ⁷ W. Han, R. K. Kawakami, M. Gmitra, and J. Fabian, *Nature Nanotechnology* **9**(10), 794–807 (2014).
- ⁸ F. Liu, L. You, K. L. Seyler, X. Li, P. Yu, J. Lin, X. Wang, J. Zhou, H. Wang, H. He, S. T. Pantelides, W. Zhou, P. Sharma, X. Xu, P. M. Ajayan, J. Wang, and Z. Liu, *Nature Communications* **7** (2016).
- ⁹ S. Jiang, J. Shan, and K. F. Mak (2018).
- ¹⁰ H. Ohno, D. Chiba, F. Matsukura, T. Omiya, E. Abe, T. Dietl, Y. Ohno, and K. Ohtani, *Nature* **408**(6815), 944–946 (2000).
- ¹¹ Y. Zhou, D. Wu, Y. Zhu, Y. Cho, Q. He, X. Yang, K. Herrera, Z. Chu, Y. Han, M. C. Downer, H. Peng, and K. Lai, - **17** (- 9), - 5513 (2017).
- ¹² Y. L. Siyuan Wan, W. Li, X. Mao, W. Zhu, and H. Zeng, *arXiv:1803.04664* (2018).
- ¹³ D. H. Keum, S. Cho, J. H. Kim, D.-H. Choe, H.-J. Sung, M. Kan, H. Kang, J.-Y. Hwang, S. W. Kim, H. Yang, K. J. Chang, and Y. H. Lee, *Nature Physics* **11**(6), 482–U144 (2015).
- ¹⁴ X. Li and J. Yang, *Journal of Materials Chemistry C* **2**(34), 7071–7076 (2014).
- ¹⁵ M.-W. Lin, H. L. Zhuang, J. Yan, T. Z. Ward, A. A. Puzos, C. M. Rouleau, Z. Gai, L. Liang, V. Meunier, B. G. Sumpter, P. Ganesh, P. R. C. Kent, D. B. Geohegan, D. G. Mandrus, and K. Xiao, *Journal of Materials Chemistry C* **4**(2), 315–322 (2016).
- ¹⁶ C. Gong, L. Li, Z. Li, H. Ji, A. Stern, Y. Xia, T. Cao, W. Bao, C. Wang, Y. Wang, Z. Q. Qiu, R. J. Cava, S. G. Louie, J. Xia, and X. Zhang, *Nature* **546**(7657), 265 (2017).
- ¹⁷ B. Huang, G. Clark, E. Navarro-Moratalla, D. R. Klein, R. Cheng, K. L. Seyler, D. Zhong, E. Schmidgall, M. A. McGuire, D. H. Cobden, W. Yao, D. Xiao, P. Jarillo-Herrero, and X. Xu, *Nature* **546**(7657), 270 (2017).
- ¹⁸ X. Zhang, Y. L. Zhao, Q. Song, S. Jia, J. Shi, and W. Han, *Jpn. J. Appl. Phys.* **55**(3), 4 (2016).
- ¹⁹ A. Soumyanarayanan, N. Reyren, A. Fert, and C. Panagopoulos, *Nature* **539**(7630), 509–517 (2016).
- ²⁰ V. Cartheaux, F. Moussa, and M. Spiesser, *Europhysics Letters* **29**(3), 251–256 (1995).